conclude whether or not the $C_6H_5B_{10}H_{13}$ they report is 6-substituted as is the isomer reported herein and that reported by Siedle et al.[8]

The new 6-substituted compounds are formed in low to moderate yields in reactions which appear complex and which are not yet fully understood. The 6-$(CH_3)_3SiOB_{10}H_{13}$ forms in reactions of $(CH_3)_3SiCl$ or $(CH_3)_3SiBr$ with $NaB_{10}H_{13}$ or $Na_2B_{10}H_{12}$ in dialkyl ethers. Other products of the reactions are H_2, C_2H_6, $[(CH_3)_3Si]_2O$, $B_{10}H_{14}$, and possibly C_2H_5Cl. In an experiment carried out so that NMR spectra could be monitored periodically, the reaction of $NaB_{10}H_{13}$ with $(CH_3)_3SiCl$ in diethyl ether showed that $[(CH_3)_3Si]_2O$ forms early in the reaction sequence, before appreciable quantities of 6-$(CH_3)_3SiOB_{10}H_{13}$ are present. However, reactions of $[(CH_3)_3Si]_2O$ with $B_{10}H_{13}^-$ or $B_{10}H_{12}^{2-}$ do not yield $(CH_3)_3SiOB_{10}H_{13}$ as a product. Also the absence of $(CH_3)_3SiOB_{10}H_{13}$ as a product in reactions of $(CH_3)_3SiCl$ with $C_2H_5OB_{10}H_{13}$ precludes direct reaction pathways. It is possible that the reaction involves initially the exchange of $(CH_3)_3Si$ for C_2H_5 groups of etherated $B_{10}H_{13}^-$ (or $B_{10}H_{12}^{2-}$), i.e., $B_{10}H_{13}O(C_2H_5)_2^-$, to form species such as $B_{10}H_{13}O$-$Si(CH_3)_3(C_2H_5)^-$ and $B_{10}H_{13}O[Si(CH_3)_3]_2^-$. Although it has been shown that the ^{11}B NMR spectrum of the $B_{10}H_{13}^-$ ion is not affected significantly by coordinating solvents,[20] solvation of $NaB_{10}H_{13}$ by ethers is well established.[21] Oxidative elimination of an ethyl group from $B_{10}H_{13}OSi(CH_3)_3(C_2H_5)^-$ could yield 6-$(CH_3)_3SiOB_{10}H_{13}$ and C_2H_6. Substitution of $(C_2H_5)_2O$ for the less basic $[(CH_3)_3Si]_2O$ on $B_{10}H_{13}$-$O[Si(CH_3)_3]_2^-$ would account for the presence of $[(CH_3)_3$-$Si]_2O$ as a reaction product. Radical processes leading to the observed products can be considered; however, products such as C_4H_{10}, $(CH_3)_3SiH$, and $[(CH_3)_3Si]_2$, which might be expected if $C_2H_5\cdot$ or $(CH_3)_3Si\cdot$ radicals were present, were not detected.

Since redistribution of alkyl groups on silicon is slow,[22] redistribution of $(CH_3)_3SiX$ to form $(CH_3)_2SiX_2$ which could then react with the decaboronate anions to form $(CH_3)_2Si$-$B_{10}H_{12}$, as occurs with alkyltin compounds, does not occur.[5,6] Also, no evidence of compounds such as $(CH_3)_3SiB_{10}H_{13}$, reported earlier by Amberger and Liedl,[23] or $[(CH_3)_3Si]_2$-$B_{10}H_{12}$ was obtained.

The 6-$C_2H_5OB_{10}H_{13}$ forms in reactions of $SnCl_4$ with $NaB_{10}H_{13}$ (or $Na_2B_{10}H_{12}$) in diethyl ether along with a lesser amount of 5-$C_2H_5OB_{10}H_{13}$.[2,3,24] This reaction may involve $SnCl_4$ as a two-electron oxidizing agent, in a role analogous to that of I_2 in $NaB_{10}H_{13}^-$–ether reactions suggested by Hawthorne and Miller.[2]

The 6-$C_2H_5OB_{10}H_{13}$:5-$C_2H_5OB_{10}H_{13}$ isomer distribution depends on the reactant combination and to a greater extent on temperature. In $NaB_{10}H_{13}$–$(C_2H_5)_2O$–$SnCl_4$ reactions, the isomer ratio varied from 85:15 to 70:30 at reaction temperatures from −112 to +25°, respectively. Previously, we showed that the product of the reaction of I_2 with $NaB_{10}H_{13}$–$(C_2H_5)_2O$ is mainly 5-$C_2H_5OB_{10}H_{13}$;[24] although from our ^{11}B NMR spectral data the presence of small amounts (5–10%) of 6-$C_2H_5OB_{10}H_{13}$ is evident. The presence of both isomeric forms in the $SnCl_4$ and I_2 reactions, along with the observation that the 6:5 ratio is temperature dependent in $SnCl_4$ reactions, suggests that the reactions may involve 5- and 6-ether-coordinated decaboronate intermediate species, though possibly not the same intermediate species since the product isomer ratios in the I_2 and $SnCl_4$ reactions are quite different. The 6-$C_2H_5OB_{10}H_{13}$–5-$C_2H_5OB_{10}H_{13}$ isomer mixture does not form as a result of the equilibration of an initially formed 5- or 6-$C_2H_5OB_{10}H_{13}$, since heating either the 5 or 6 isomer for prolonged periods of time produces no detectable isomerization.

The $C_6H_5B_{10}H_{13}$ forms during the thermal decomposition of $(C_6H_5)_2SnB_{10}H_{12}$, along with substantial amounts of $B_{10}H_{14}$. No other products have been isolated. Although $(C_6H_5)_2SnB_{10}H_{12}$ is too unstable to allow isolation from small amounts of coformed phenyltin chloride products, its spectral properties allow it to be adequately characterized as an aryl analogue of the previously reported dialkylstannaundecaboranes[5,6] and to be confirmed as the source of 6-$C_6H_5B_{10}H_{13}$. The thermal instability of $(C_6H_5)_2SnB_{10}H_{12}$ is in striking contrast to that of the dialkyl compounds, where heating at 60° for sustained periods causes only slight decomposition. It is interesting to note that no aryltin–decaborane products were isolated from reactions of $(C_6H_5)_2SnCl_2$ with $[(C_6H_5)_4As]_2B_{10}H_{12}$.[25]

Registry No. $(CH_3)_3SiCl$, 75-77-4; $Na_2B_{10}H_{12}$, 12046-70-7; $NaB_{10}H_{13}$, 12008-65-0; 6-$(CH_3)_3SiOB_{10}H_{13}$, 57527-18-1; $SnCl_4$, 7646-78-8; $(C_2H_5)_2O$, 60-29-7; 6-$C_2H_5OB_{10}H_{13}$, 57527-19-2; $(C_6H_5)_2SnCl_2$, 1135-99-5; $(C_6H_5)_2SnB_{10}H_{12}$, 57527-53-4; 6-$C_6H_5B_{10}H_{13}$, 38998-69-5.

References and Notes

(1) This work was supported by National Science Foundation Grants GP-8090 and GP-23575.
(2) M. F. Hawthorne and J. J. Miller, *J. Am. Chem. Soc.*, **82**, 500 (1960).
(3) R. F. J. Palchak, J. H. Norman, and R. E. Williams, *J. Am. Chem. Soc.*, **83**, 3380 (1961).
(4) J. Plesek, S. Hermanek, and B. Stibr, *Collect. Czech. Chem. Commun.*, **33**, 691 (1968).
(5) R. E. Loffredo and A. D. Norman, *J. Am. Chem. Soc.*, **93**, 5587 (1971).
(6) R. E. Loffredo, A. D. Norman, and R. Schaeffer, submitted for publication.
(7) F. Hanousek, B. Stibr, S. Hermanek, J. Plesek, A. Vitek, and F. Haruda, *Collect. Czech. Chem. Commun.*, **37**, 3001 (1972).
(8) A. R. Siedle, D. McDowell, and L. J. Todd, *Inorg. Chem.*, **13**, 2734 (1974).
(9) H. Gilman and L. A. Gist, Jr., *J. Org. Chem.*, **32**, 368 (1967).
(10) J. J. Miller and M. F. Hawthorne, *J. Am. Chem. Soc.*, **81**, 4501 (1959).
(11) P. H. Wilks and J. C. Carter, *J. Am. Chem. Soc.*, **88**, 3441 (1966).
(12) Elemental analyses performed by Schwarzkopf Microanalytical Laboratories, Woodside, N.Y.
(13) D. F. Shriver, "The Manipulation of Air-Sensitive Compounds", McGraw-Hill, New York, N.Y., 1969.
(14) Spectrum superimposable with sample of known material from a laboratory supply.
(15) N. Wright and M. J. Hunter, *J. Am. Chem. Soc.*, **69**, 803 (1947).
(16) J. W. Emsley, J. Feeney, and L. H. Sutcliffe, "High-Resolution Nuclear Magnetic Resonance Spectroscopy", Vol. 2, Pergamon Press, Oxford, 1966.
(17) H. A. Szymanski, "Infrared Band Handbook", Plenum Press, New York, N.Y., 1963.
(18) S. Hermanek, J. Plesek, and V. Gregor, *Collect. Czech. Chem. Commun.*, **31**, 1281 (1966).
(19) R. F. Sprecher, B. E. Aufderheide, G. W. Luther III, and J. C. Carter, *J. Am. Chem. Soc.*, **96**, 4404 (1974), and references cited therein.
(20) A. R. Siedle, G. M. Bodner, and L. J. Todd, *J. Inorg. Nucl. Chem.*, **33**, 3671 (1971).
(21) N. J. Blay, R. J. Pace, and R. L. Williams, *J. Chem. Soc.*, 3416 (1962).
(22) E. A. V. Ebsworth, "Volatile Silicon Compounds", Pergamon Press, New York, N.Y., 1963.
(23) E. Amberger and P. Leidl, *J. Organomet. Chem.*, **18**, 345 (1969).
(24) A. D. Norman and S. L. Rosell, *Inorg. Chem.*, **8**, 2818 (1969).
(25) N. N. Greenwood and B. Youll, *J. Chem. Soc., Dalton Trans.*, 158 (1975).

Contribution from the Inorganic Chemistry Laboratory, University of Oxford, Oxford OX1 3QR, England

Investigation of the Structure of Barium Iridate ($BaIrO_3$) by High-Resolution Electron Microscopy

P. L. Gai, A. J. Jacobson, and C. N. R. Rao*[1]

Received July 22, 1975 AIC50531Q

Donohue, Katz, and Ward[2] suggested that the structure of barium iridate, $BaIrO_3$, was based on a nine-layer stacking of BaO_3 layers in the sequence $(chh)_3$ similar to the rhombohedral phase of $BaRuO_3$ (a = 5.75 Å, c = 21.6 Å). The transition metal ions are in strings of three face-shared MO_6 octahedra which are corner linked.[3,4] However, in order to

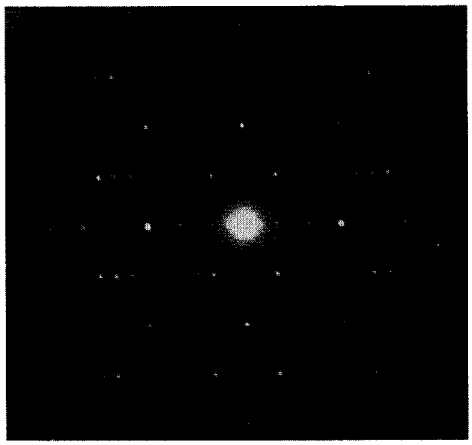

Figure 1. Electron diffraction pattern of 9H-$BaIrO_3$ with the beam along $\langle 10\bar{1}0 \rangle$.

Figure 2. Electron diffraction pattern of 9R-$BaRuO_3$ with the beam along $\langle 10\bar{1}0 \rangle$.

establish the correspondence, 50 weak $h0l$ reflections were ignored in a structure refinement based on single-crystal x-ray data. The weak extra reflections could be indexed with a doubled hexagonal c axis of 44.4 Å and intensities of the $hk0$ reflections indicated that the true symmetry was lower than hexagonal. Rodi and Babel[5] had earlier suggested an 18-layer rhombohedral cell with c = 44.5 Å for this compound.

To investigate the structure of $BaIrO_3$, we have employed the technique of lattice imaging by electron microscopy in conjunction with electron diffraction as well as x-ray powder diffraction. In favorable circumstances, the electron microscope can be used to generate from a thin crystal an image which closely resembles the projected structure.[6] This direct method of structure investigation has been particularly effective in examining the niobium oxide "block" structures and other materials with a relatively open network of octahedra.[6,7] In more closely packed systems where the projected charge density is less simple, only a few systems like hexagonal ferrites,[8] perovskites[9] and silicon carbide[10] have been recently examined by this technique. In particular, it has been shown that perovskite polytypes with Ba^{2+} as the A cation give projected charge densities which may be correlated directly with the stacking of the BaO_3 layers. Lattice images of these perovskite polytypes show chevrons corresponding to columns of Ba cations and BO_6 octahedra which alternate in direction wherever there is a hexagonally close-packed layer.[9,11] Thus, in the lattice image of a 4H (chch stacking) perovskite polytype, the chevrons show reversal of slope every alternate layer.[11] It, therefore, appeared to us that the $BaIrO_3$ system might be a suitable case to test the lattice imaging technique for use in direct structure determination of unknown structures. It should be noted also that the strong scattering of electrons in diffraction may give extra sensitivity to superstructure reflections compared with the x-ray technique.

Experimental Section

$BaIrO_3$ and $BaRuO_3$ were prepared by the reaction of BaO_2 and Ir or Ru metal at 1000°C in air.[2,4] A sample of 4H-$BaCrO_3$ prepared by high-pressure synthesis[12] was provided by Professor Chamberland.

A Siemens Elmiskop 102 electron microscope was used with an accelerating voltage of 100 kV to obtain micrographs. Thin crystals from a finely ground powder sample of $BaIrO_3$ were mounted on carbon-coated copper grids and orientated by means of a ±45° double-tilt stage. A 50-μ objective aperture was used to combine the primary beam with superlattice and subcell reflections out to about 3 nm^{-1} and micrographs were recorded with the electron beam parallel to $\langle 10\bar{1}0 \rangle$ and $\langle 0001 \rangle$ in a through-focus series embracing the optimum condition. The image magnifications were 300000× and 500000×. The specimens being beam sensitive caused some difficulties in microscopy.

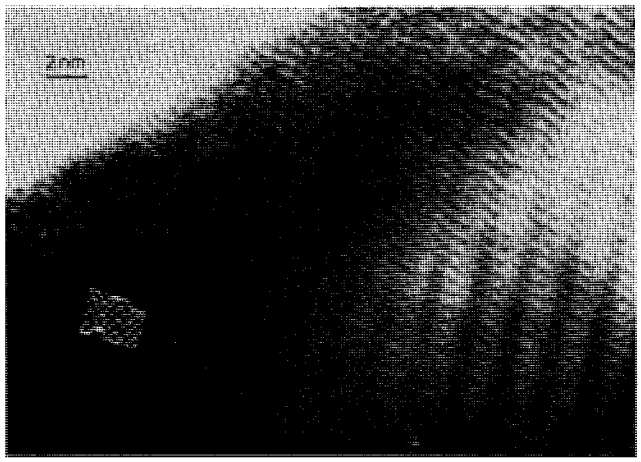

Figure 3. Lattice image of 9H-$BaIrO_3$ with an idealized (2)3(1)3 insert.

Powder x-ray diffraction patterns were obtained with a Philips wide-angle goniometer and monochromated Cu Kα radiation and with a Guinier camera.

Results and Discussion

Electron microscopy of selected crystals of $BaIrO_3$ revealed several unusual features. Some crystals gave diffraction patterns which correspond to a nine-layer sequence of BaO_3 layers with unit cell parameters a = 5.80 Å and c = 22.15 Å in reasonable agreement with those reported by Donohue et at.[2] (a = 5.76 Å, c = 22.2 Å). The electron diffraction pattern shown in Figure 1 indicates that the symmetry is hexagonal and not rhombohedral as found for 9R-$BaRuO_3$.[11] The corresponding electron diffraction pattern of $BaRuO_3$ is given in Figure 2 for comparison. This pattern clearly shows rhombohedral absences ($-h + k + l = 3n$) in the $0kl$ section of the pattern. Rotation of the $BaIrO_3$ crystals about the electron beam confirmed that the extra reflections were not a consequence of multiple diffraction effects but were genuine reflections of the 9H phase. The lattice image of this 9H phase of $BaIrO_3$ is shown in Figure 3 and discussed further below. It may be pointed out that 9R-$BaRuO_3$ does not give a high-resolution lattice image because of the rhombohedral absences.[11] As such, the lattice image of $BaRuO_3$ cannot be used to obtain information on the stacking sequence.

Several crystals of $BaIrO_3$ examined gave lattice images which showed the presence of both the 9H structure and a second phase shown in Figure 4. The second phase can be

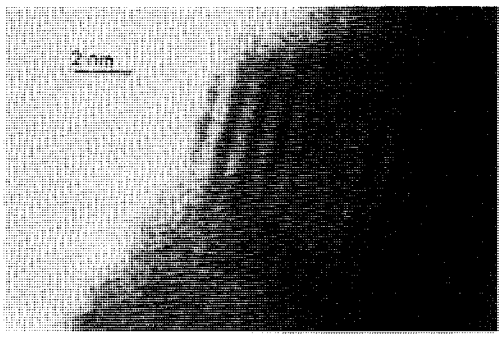

Figure 4. Lattice image of $BaIrO_3$ showing domains of 4H.

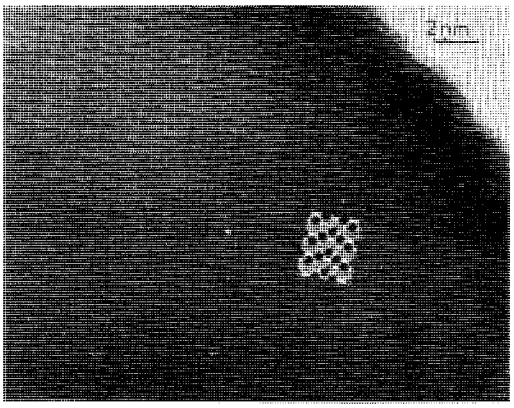

Figure 5. Lattice image of 4H-$BaCrO_3$ with the inset showing the $(ch)_2$ sequence.

identified as a four-layer sequence $(ch)_2$ by comparison with the lattice image of 4H-$BaCrO_3$ (Figure 5).[11,12] We see the slope reversal of chevrons at every alternate layer 4.7 Å apart as expected of the chch sequence. The domain size of the 9H and 4H phases in $BaIrO_3$ was about 200 Å. The presence of the four-layer structure is not unreasonable since $BaRuO_3$ is known to transform to 4H at high temperature.[11] It seems likely that the difficulty experienced by Donohue et al.[2] in indexing the x-ray data for $BaIrO_3$ may have been partly due to the presence of a two-phase mixture of four- and nine-layer structures. Occurrence of several polytypic phases of a perovskite is well documented in the literature. Thus, $BaMnO_3$ which has the two-layer sequence at ordinary temperatures, gives rise to several anion-deficient polytypes with increase in temperature with the six-layer form itself existing in two different forms.[13]

Examination of the powder x-ray diffraction pattern of $BaIrO_3$ revealed results essentially similar to those of Donohue et al.[2] The nine-layer reflections satisfying the rhombohedral condition, $-h + k + l = 3n$, are strong but there are in addition a considerable number of weaker reflections which cannot all be indexed by doubling the hexagonal c axis. In particular, two low-angle reflections with $d = 5.627$ and 5.155 Å suggest that enlargement of the basic nine-layer hexagonal cell to an orthorhombic superstructure is required. However, because electron microscopy reveals the presence of two phases and also because the resulting cell would be very large, it was not considered practicable to index the diffraction pattern completely. Also, it was not possible to obtain electron diffraction patterns of the $hk0$ net to verify any basal plane superstructure for the 9H phase. Furthermore, there was no evidence for c-axis doubling in the electron diffraction results.

For hexagonal stacking of nine BaO_3 layers, six possibilities exist. Each of these has been examined and compared with the lattice image (Figure 3). Only two of the sequences would be expected to give charge density projections similar to the observed lattice image. These may be described in Zhdanov notation as 4221 and (2)3 (1)3 or cchchchhc and hchcchhcc. Both of these sequences contain elements of the 4H structure, namely, chch (i.e., pairs of face-shared octahedra corner linked) and elements of the 9R-$BaRuO_3$ structure, chh (strings of three face-shared octahedra). The inset in Figure 3 is an idealized projection of (2)3 (1)3. Comparison of this projection with the image suggests that (2)3 (1)3 is the most likely structure although it is not possible to be absolutely certain on this point. The 9H structure of $BaIrO_3$ is indeed novel in that it is the first known example of a 9H perovskite polytype.

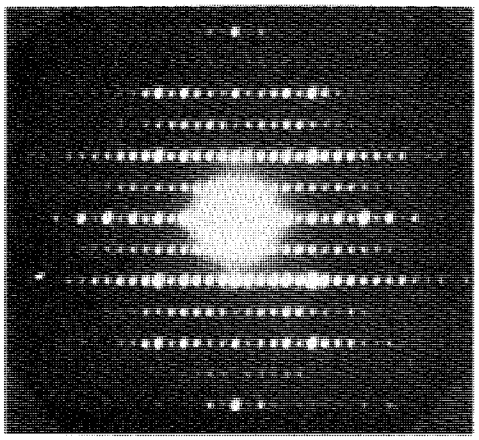

Figure 6. $(h0l)$ electron diffraction pattern of $BaIrO_3$ heated to 1400°C.

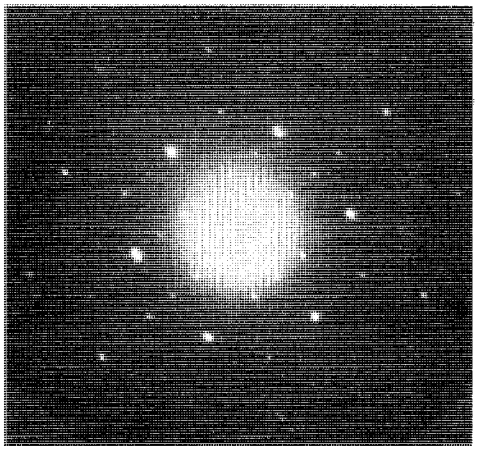

Figure 7. $(hk0)$ electron diffraction pattern of $BaIrO_3$ heated to 1400°C.

The sample of $BaIrO_3$ prepared at 1000°C was heated at 1400°C for 3 days in air and quenched in the hope of obtaining a single-phase product. Electron diffraction patterns were obtained with the electron beam along $\langle 10\bar{1}0 \rangle$. All crystals examined gave patterns corresponding to a nine-layer sequence of BaO_3 layers with a c-axis dimension of 21.2 Å, somewhat shorter than found for the 1000°C sample (22.15 Å). In addition, in all cases, the a axis was found to be doubled (Figure 6). It also proved possible to obtain for this sample diffraction patterns with the electron beam along $\langle 0001 \rangle$. Examination of these patterns (Figure 7) revealed that the superlattice is orthorhombic rather than hexagonal with cell parameters related to the simple hexagonal cell by $a \approx 2a_{hex}$, $b \approx 2(3^{1/2})a_{hex}$, $c = c_{hex}$. Powder x-ray patterns could be completely indexed on this cell with lattice parameters, $a =$

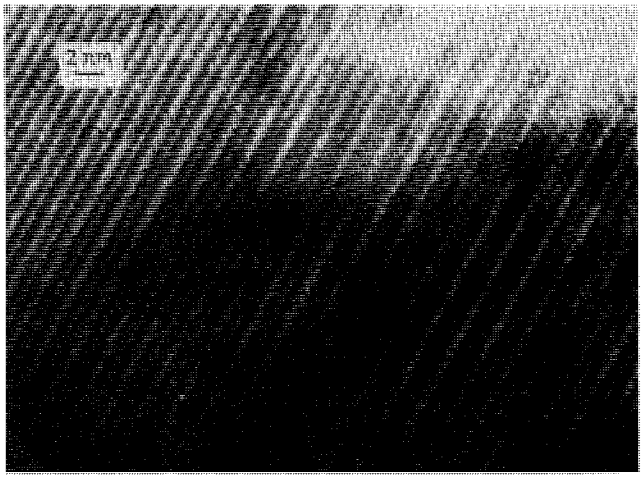

Figure 8. Lattice image of $BaIrO_3$ heated to 1400°C. This is somewhat similar to the image shown in Figure 3, but it has not been possible to analyze the detailed features of this image.

11.8, b = 20.4, and c = 21.2 Å. Lattice images of this high-temperature sample (Figure 8) were qualitatively similar to those of the 9H low-temperature phase but contained much more detail.

The reasons for the formation of the superstructure and for the c-axis contraction are not yet clear. However, we may note that 6H-$SrIrO_3$ has a monoclinic distortion of an orthorhombic supercell[14] based on $a \approx a_{hex}$ and $b = 3b_{hex}$. It is possible that the c-axis shortening may arise from some reduction of $BaIrO_3$ when it is heated to 1400°C. $SrIrO_3$ is known to undergo reduction in hydrogen below 400°C to give Sr_2IrO_4 together with Ir metal. While we do not have a clear explanation for the c-axis shortening or for the superstructure formation when $BaIrO_3$ is heated to 1400°C, the structural features found by us for the high-temperature phase provide an interesting comparison to those of the low-temperature 9H phase. It is possible that some of the weak reflections in the x-ray pattern of the low-temperature phase could arise from the presence of the high-temperature phase. However, more detailed studies of $BaIrO_3$ as a function of temperature would be necessary before we fully understand the transformations in the 1000–1400°C range.

Acknowledgment. The authors are grateful to Professor J. S. Anderson for the use of the electron microscope and for his interest in this work and to Professor B. L. Chamberland for providing a sample of 4H-$BaCrO_3$.

Registry No. $BaIrO_3$, 12230-76-1.

References and Notes

(1) Commonwealth Visiting Professor, University of Oxford, 1974–1975. Correspondence should be addressed to Department of Chemistry, Indian Institute of Technology, Kanpur 208016, India.
(2) P. C. Donohue, L. Katz, and R. Ward, *Inorg. Chem.*, **5**, 335 (1966).
(3) J. J. Randall and R. Ward, *J. Am. Chem. Soc.*, **81**, 2629 (1959).
(4) P. C. Donohue, L. Katz, and R. Ward, *Inorg. Chem.*, **4**, 306 (1965).
(5) F. Rodi and D. Babel, *Z. Anorg. Allg. Chem.*, **336**, 17 (1965).
(6) J. G. Alpress and J. V. Sanders, *J. Appl. Crystallogr.*, **6**, 165 (1973).
(7) J. M. Cowley and S. Iijima, *Z. Naturforsch., A*, **27**, 445 (1972); J. L. Hutchison and J. S. Anderson, *Phys. Status Solidi A*, **9**, 207 (1972).
(8) J. D. M. McConnell, J. L. Hutchison, and J. S. Anderson, *Proc. R. Soc. London, Ser. A*, **339**, 1 (1974).
(9) J. L. Hutchison and A. J. Jacobson, *Acta Crystallogr., Sect. B*, **31**, 1442 (1975).
(10) P. L. Gai, J. S. Anderson, and C. N. R. Rao, *J. Phys. D*, **8**, 157 (1975).
(11) P. L. Gai and C. N. R. Rao, submitted for publication.
(12) B. L. Chamberland, *Inorg. Chem.*, **8**, 286 (1969).
(13) T. Negas and R. S. Roth, *J. Solid State Chem.*, **3**, 323 (1971).
(14) J. M. Longo, J. A. Kafalas, and R. J. Arnott, *J. Solid State Chem.*, **3**, 174 (1971).

Contribution from the Department of Chemistry, Ithaca College, Ithaca, New York 14850

Binding of Pyridine to Phenyl-Substituted Derivatives of Zinc Tetraphenylporphine

Glenn C. Vogel* and Bruce A. Beckmann[1]

Received July 28, 1975 AIC50542J

The binding of nitrogenous donors to metalloporphyrins has been studied in great detail.[2] Recently the adduct formation between zinc tetraphenylporphine and oxygen, sulfur, and phosphorus donors has been reported.[3] However, only a few studies have been reported in which the donor is held constant and the metalloporphyrin is changed gradually by varying the peripheral groups.[4] In this work the binding of pyridine to a series of m-phenyl- and p-phenyl-substituted derivatives of zinc tetraphenylporphine, Zn(m- or p-X)TPP, in the solvent benzene is reported.

Experimental Section

The phenyl-substituted tetraphenylporphines and the corresponding zinc porphyrins were synthesized by literature methods.[5,6] The zinc porphyrins were purified by dry-column chromatography.[3,6] Aldrich pyridine was purified as reported[7] and Baker Analyzed reagent benzene was treated as reported.[8] The absorbance measurements were made on a Cary Model 14 uv–visible spectrophotometer with a thermostated cell compartment. All measurements were made at 25° using quartz cells with 1-cm path length. All systems were studied at four different wavelengths and the spectral data for all the systems are listed in Table I available in the microfilm edition. The procedure for the treatment of the data has been reported.[3]

Results and Discussion

Table II contains the extinction coefficients of the phenyl-substituted zinc porphyrins prepared for this study, the substituent constants (σX), and log K where K is the equilibrium constant for the formation of the 1:1 adduct between pyridine and a zinc porphyrin. Figure 1 is a plot of log K vs 4σX. Both the meta and para derivatives have been plotted on the same figure. In general, there is an increase in the binding of pyridine by the zinc porphyrin with increasing electron-withdrawing character of the substituent. Two metalloporphyrins deviate substantially from the least-squares line, ZnTPP and Zn(m-OCH_3)TPP. Examination of data from a recent study[4d] of the binding of piperidine to a series of m-phenyl- and p-phenyl-substituted derivatives of nickel tetraphenylporphine, Ni(m- or p-X)TPP, shows that the m-OCH_3 derivative for this system has a lower equilibrium constant toward piperidine than would be predicted from a least-squares line for the data of the other derivatives. A similar result is displayed in Figure 1. The determination of equilibrium constant for ZnTPP has been repeated several times and the results are the same within experimental error. Two other studies of the ZnTPP–py system have been reported[9,10] and data from these studies are presented in Table II and Figure 1.

The slope of the line in Figure 1 omitting the H and m-OCH_3 points is 0.188 ± 0.007. Similar plots for the VO(p-X)TPP–piperidine system and the Ni(p-X)TPP–piperidine[4d] system gave slopes of 0.113 ± 0.003 and 0.331 ± 0.005, respectively. Assuming no major differences occur in the mode of transmission of the electronic effects because of the different donors (pyridine vs. piperidine) and different solvents (benzene vs. toluene) used in this and the other study,[4d] it appears that the Zn(m- or p-X)TPP series is more sensitive to change on the periphery of the molecule than the VO(p-X)TPP series but less sensitive than the Ni(p-X)TPP series.

It has been suggested that the VO(p-X)TPP series is less sensitive to substituent changes than the Ni(m- or p-X)TPP